

A Narrowband Low-Profile Second-Order Bandpass Frequency Selective Surface Using Third Harmonics

Muaad Hussein, Yi Huang, Abed Sohrab, Muayad Kod, Jiafeng Zhou

Abstract—In high-order ($N > 1$) frequency selective surfaces (FSSs), the surfaces are usually cascaded vertically and separated by a dielectric substrate to achieve desired responses. The dielectric substrate thickness is a critical parameter in designing such structures. It is usually high for most traditional designs. In this paper, we present a novel approach for designing extremely low-profile high-order bandpass FSSs. The structure is built by using the coupling of the third harmonics instead of the fundamentals of the resonators to achieve a bandpass response. By using the proposed design method, the coupling between the third harmonics can be very weak with a very thin substrate, and a flat response can be achieved. The overall thickness of a second-order FSS can be reduced to $\lambda/75$, where λ is the free space wavelength. A prototype of the proposed bandpass FSS is designed, fabricated, and experimentally characterized. The measurement results of this device show a very good and stable frequency response with respect to the angle of incidence up to $\pm 45^\circ$ as predicted.

Index Terms—Frequency selective surface, low profile, bandpass FSS, second order, third harmonics

I. INTRODUCTION

THE defining feature of a frequency selective surface (FSS) is its ability to act as a surface with bandpass or bandstop filtering properties to incident waves. This is accomplished through a periodic array of conductive elements that capacitively or inductively coupled when excited by incident electromagnetic waves (e.g., a plane wave).

The FSSs may be active, featuring amplification structures, or completely passive. There may be connecting structures, such as vias, between FSS layers or each FSS layer may be electrically isolated [1-4].

Highly selective filtering and narrowband performances are required in certain applications. As spatial filters, FSSs can be used to reduce the radar cross sections (RCS) of objects mounted on stealthy platforms [1] and shield sensitive electronic devices from unwanted signals. FSSs with narrow bandwidths and high selectivity can be used to sufficiently attenuate strong out-of-band interference/jamming signals.

Many different techniques have been used to design high (greater than 1) order FSSs. In [5], non-resonant traditional patch and wire grid surfaces were used to design a low-profile second-order bandpass FSS. The size of the array element of this structure is miniaturised by increasing the capacitance value. This is done by using interdigital capacitive patches for the first

and third layer. The element size of this structure when using patches is $0.19\lambda \times 0.19\lambda$ with a thickness of $\lambda/25$. Or it is $0.15\lambda \times 0.15\lambda$ with a thickness of $\lambda/30$ after using the interdigital capacitive structures.

A miniaturized dual-band FSS with a second-order bandpass response at each operation band is designed by cascading a two-dimensional periodic array of double square loops and an array of wire grids. The overall thickness at the first band is about $\lambda/15$, as in [6]. An inductively coupled FSS that uses capacitively loaded dielectric spacers as its main resonators is introduced in [7]. A miniaturized surface making use of couplings between inductive surfaces to design a third order single polarization bandpass is demonstrated in [8], where the overall thickness is $\lambda/3.89$. In [9], a high-order bandpass FSS as designed by using inductively coupled miniaturized elements. The structure exhibits a narrow bandpass response with an overall thickness of $\lambda/3.75$.

In this paper, a novel approach to build a second-order FSS with a low profile is proposed. This approach is based on the use of the third harmonic of a resonant structure instead of the fundamental mode. In doing so, an extremely low-profile second-order bandpass FSS can be designed, where the overall thickness of the FSS can be reduced to around $\lambda/75$ and even further. The structure exhibits a low-loss transmission coefficient. By using the proposed approach, the design of low-profile high-order FSSs is achievable. The detailed design process, simulated and measured results are given in the following sections. Discussion and conclusions are presented in the final section.

II. RESONANT STRUCTURE

There are different ways to develop bandpass filters. One commonly used method is to use multiple resonators tuned at the same frequency. If these resonators are coupled to each other with suitable coupling coefficients, and coupled to the source and load with proper external quality factors, a bandpass response can be obtained [10]. Conventionally, the resonators operate at their fundamental frequencies. However, the same design method is still valid if the resonators operate at other harmonic frequencies. In this paper, the thicknesses of dielectric substrate layers, which are used to separate metallic surfaces of an FSS, is reduced by using the third harmonic of the resonant surface as the main operation mode. In the proposed structure, two half-wavelength (λ_g) resonators are coupled by an inductive surface, where λ_g is the guided

wavelength ($\lambda_g = \lambda/\sqrt{\epsilon_r}$) at the fundamental frequency, and ϵ_r is the effective dielectric constant of the substrate. A half-wavelength FSS resonator resonates at an odd number times of the fundamental frequency (f_0), i.e., $(2n - 1)f_0$ with $n = 1, 2, 3 \dots$ where f_0 is the fundamental resonating frequency of the FSS [1]. In this study, it will be demonstrated how to enhance the third harmonic of a resonator and how to design extreme low-profile second-order FSS with such resonators. A compact structure was introduced in [11] to design second-order FSSs with miniaturized elements. This structure is adapted in this paper as example to design an extremely low profile second-order FSS. The first and third surfaces are identical. Each array element is formed by a square loop with four stepped-impedance transmission lines. The middle surface is built by using grids to provide inductance. Two dielectric slabs (FR-4) with a dielectric constant of 4.3 are used to separate the two resonating surfaces and the inductive surface. The dielectric slabs can be represented by two short pieces of transmission lines with a thickness of h . The characteristic impedance of the dielectric slab is $Z_d = Z_0/\sqrt{\epsilon_r}$, where ϵ_r is the dielectric constant of the substrates. Z_0 is the free space intrinsic impedance. This circuit is a second-order coupled-resonator bandpass filter [12]. Fig. 1 shows the geometry dimensions of different layers of the FSS. Each array element has maximum physical dimensions of P in the x and y directions, respectively, which are also the same as the period of the grid in the x and y directions. The inductive layer is of the form of two metallic strips crossing to each other with a size of $P \times P$, and width of w_i . D is the periodic element in the x and y directions of the resonator (first and third layer) and equal to $P-S$, where S is the gap width between adjacent elements. w_p is the width of the square patches inside the square ring; w_s is the width of the strips inside the square ring; w_l is the width of the square ring perimeter. For normal incident waves, the equivalent circuit as shown in Fig. 2 can be used to explain the operation principles of the proposed structure. In Fig. 2, C_1 represents the mutual capacitance between adjacent elements in the resonator layer. C_2 represents the capacitance between the patches of an element in the resonator. L_1 represents the inductance of the outer lines of the resonator surface. L represents the inductance of the middle (inductive) layer inductor. To design the proposed FSS with the desired response, one can first determine the values of the elements used in the equivalent circuit model of Fig. 2, then the initial dimensions of these LC components can be

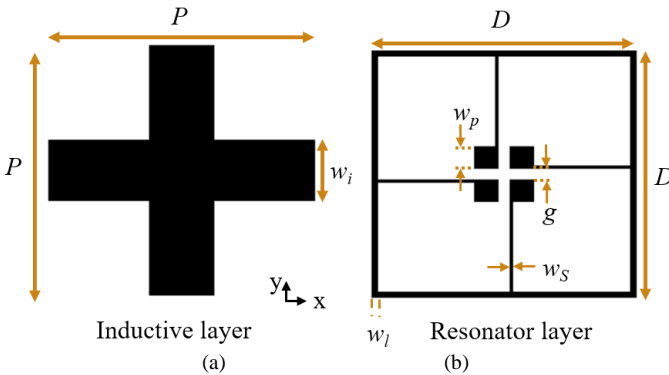


Fig. 1. Top view of the array elements of the second-order bandpass FSS: (a) the inductive (grid) surface layer and (b) the resonant element.

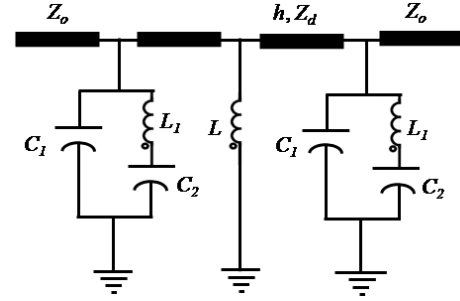


Fig. 2. Equivalent circuit model of the proposed second-order bandpass FSS.

Table I: Dimensions of the element of the proposed second-order bandpass FSS, the unit is mm

Parameter	P	D	w_l	h_1	g
Value	18	17.8	0.4	0.8	0.8
Parameter	w_s	w_i	w_p	h_2	
Value	0.2	4.4	1.6	0.8	

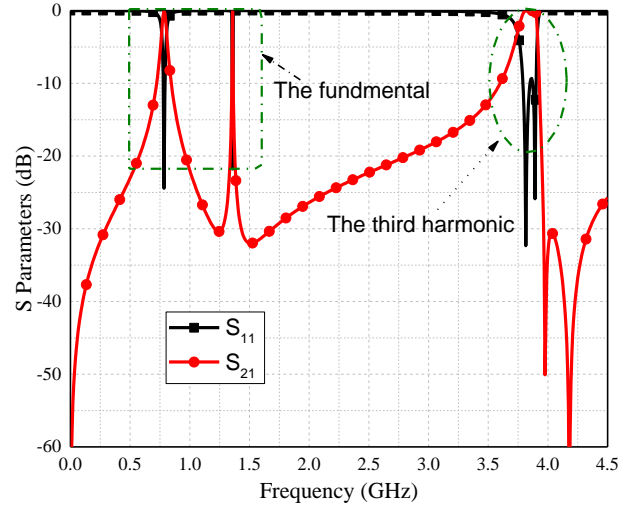


Fig. 3. Simulated magnitudes of transmission and reflection coefficients of the proposed FSS with a very thin substrate.

approximated using the formulas in [13]. Finally, dimensions of the FSS structure are obtained using a full-wave simulation tool, CST Microwave Studio, to achieve the desired frequency response. The final design parameters of the structure and its unit cell are listed in Table I. Fig. 3 shows the simulated frequency response of the proposed FSS for normal incident waves. It can be observed that a flat bandpass response is achieved at the third harmonic frequency (3.78 GHz-3.96 GHz), while two peaks can be observed at the fundamental frequency (0.76 GHz and 1.35 GHz). This is because with a thin substrate the coupling between the first and the third layer is very strong at the fundamental frequency. Thus, although the coupling through the effective transmission line (h_1+h_2) is weakened by the shunt inductance L of the middle layer, the direct coupling between the first and third layers is still very strong and will introduce two peaks around the fundamental frequency. It will be explained below that at the third harmonic, the coupling between the two resonators at the third harmonic frequency is much weaker. This can be observed from the current distribution on the FSS surfaces as shown in Fig. 4. At the fundamental frequency, the current is mainly distributed on the square rings of the first and third layers, as can be seen from

Fig. 4(a) and (b). The coupling between these two layers is very strong. At the third harmonic, the current is mainly distributed around the center of the rings on both sides and on two of the four step-impedance transmission lines inside the square ring, as shown in Fig. 4(c). The couplings between the first and third layers at these three parts would have been very strong. However, due to the design, there are metallic strips at the same places in the middle layer. The middle layer will significantly weaken the coupling. Accordingly, a flat bandpass response can be achieved. In this design, the center frequency of the third-harmonic passband is at 3.9 GHz. The fractional bandwidth is 4.6%. The simulated insertion loss at the passband is 0.12 dB at the normal incident angle. The structure exhibits an excellent second-order response even with a reduced substrate thickness. The structure is simulated with different substrate thicknesses while other parameters are provided in Table I. Fig. 5 shows the simulated results of the structure with three different substrate thicknesses (h_1 and h_2). It can be observed that the structure still exhibits an excellent second-order bandpass response with a substrate thickness equal to as thin as $\lambda/75$, $h_1 = h_2 = 0.5$ mm. The thickness could be further decreased by optimizing the structure on the middle layer.

The proposed FSS element was designed to be rotationally symmetrical around Z-axis. For this reason, its response is almost independent from the polarization angle. The structure was simulated under various incident angles. The resonant frequency and the bandwidth of an FSS are usually affected by the incident angle. These effects are mainly due to the fact that the values of the inductance and capacitance of an FSS depend not only on the polarisation angle but also on the angle of incidence (θ). The results indicate that the response is very stable under 0° , 15° , 30° and 45° incident angles, as shown in Fig. 6. The variation in the bandwidth of the structure as the angle of incidence varies can be attributed to the change of wave impedance, which will change the loaded quality factor of a resonator in an FSS structure. For the TE mode, the wave impedance changes to $Z_0/\cos(\theta)$ [14], where θ is the incident angle. Therefore, in the case of a large incident angle, the wave impedance increases, and the bandwidth decreases for parallel resonators because the loaded equality factor Q_L increases, while the bandwidth increases for a series resonator. For TM mode, the wave impedance changes to $Z_0 \cos(\theta)$ [14]. For this reason, Q_L decreases for large incident angles, and consequently the bandwidth increases for parallel resonators, or decreases for series resonators. The proposed structure has been fabricated and tested to validate the design. The fabricated FSS is shown in Fig. 7. The dimensions of the FSS prototype are $216 \text{ mm} \times 216 \text{ mm}$. It consists of 12×12 elements on FR4 substrate. A vector network analyzer and two horn antennas were used for the test. Two steps were used in the measurement procedure. First, in the free space case, the transmission coefficient between the two horn antennas was measured without the FSS. Second, the transmission coefficient was measured again with the FSS prototype between the antennas. Then the measured transmission coefficient with the FSS is normalized with respect to the measured data without the FSS.

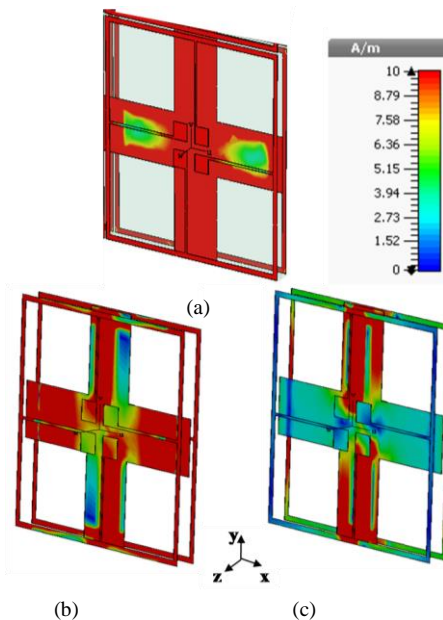


Fig. 4. Current distribution of the proposed structure: (a) at 0.75 GHz, (b) at 1.4 GHz and (c) at 3.9 GHz.

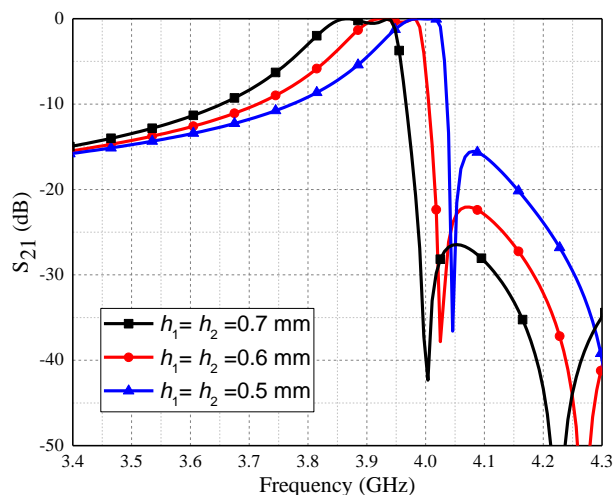


Fig. 5. Simulated transmission coefficients of the structure at the third harmonic with different substrate thicknesses.

The distance is large enough to satisfy the far field condition (meeting $> 2D^2/\lambda$ condition), where D is the antenna aperture size and λ is the wavelength in free space at the resonant frequency. The transmission coefficient S_{21} was measured at various angles of incidence. The measured results are shown in Fig. 7 for the incident angles of 0° and 30° . They show very good agreement with the simulated ones. The measured results for incident angles of 15° and 45° are also in good agreement with simulation but were not shown in Fig. 8.

The discrepancy between the simulation and measurement results is mainly attributed to the tolerances involved in the fabrication process, inaccuracies in the exact values of the parameters of the dielectric substrates used, and the small deviation due to the scattering from the stand used to hold the FSS.

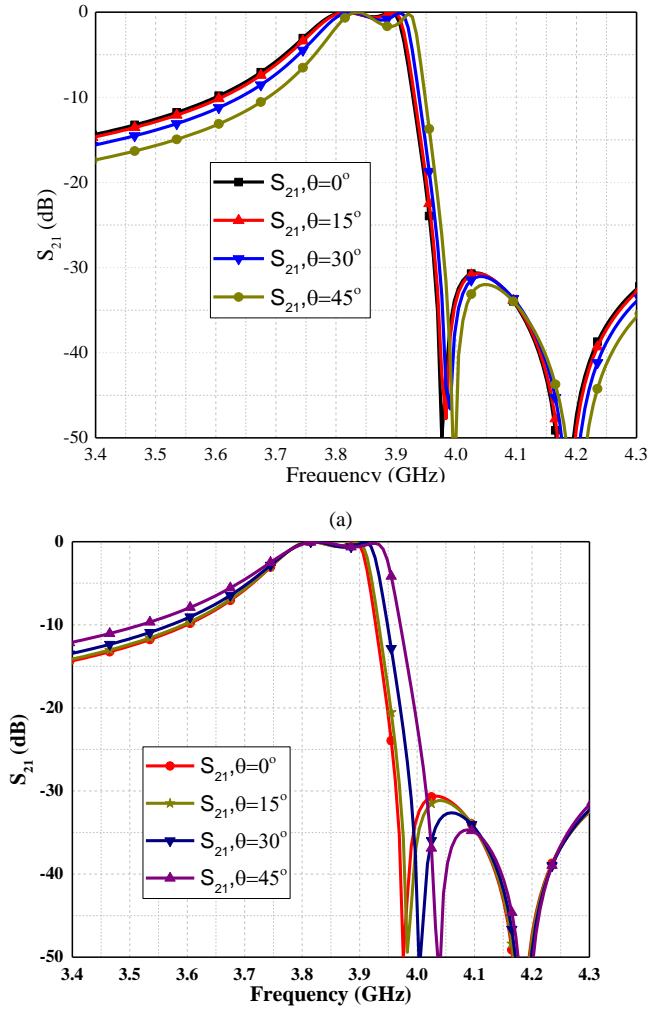


Fig. 6. Simulated transmission coefficients of the proposed second-order FSS with varied incident angles, (a) TE mode response, (b) TM mode response.

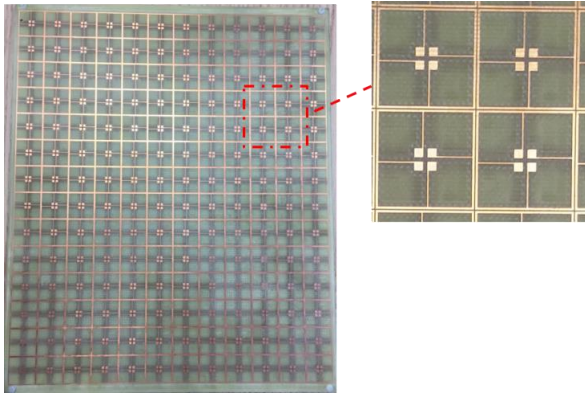


Fig. 7. Photograph of the prototype of the proposed FSS.

As can be seen from Fig. 7, a bandpass response is exhibited at the third harmonic. The center frequency of the passband is 3.86 GHz with a fractional bandwidth of 4.4%. The proposed FSS exhibits insensitive frequency response to the angle of incident wave up to $\pm 45^\circ$.

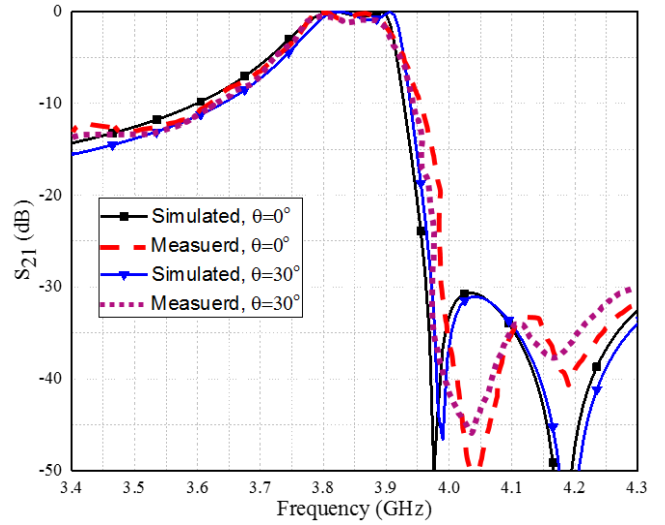


Fig. 8. Measured and simulated transmission coefficients of the proposed FSS at the third harmonic.

A comparison of the proposed FSS filter with other reported ones is illustrated in Table II. It can be seen that the proposed structure has the thinnest profile.

Table II. Comparison of the proposed FSS with other works regarding the thickness of substrate and fractional bandwidth (BW).

FSS	Order	f_o (GHz)	Overall thickness	BW
[5]	2	10	0.033λ	20%
[6]	2	10	0.067λ	21%
[7]	2	16.5	0.22λ	10%
[8]	3	8.5	0.257λ	15%
[9]	2	21	0.273λ	5%
This FSS	2	3.9	0.013λ	4.6%

III. DISCUSSION AND CONCLUSIONS

In this paper, a novel technique to design high-order bandpass FSSs with extremely thin dielectric substrates has been introduced. The proposed structure is built based on the coupling between the third harmonics of resonant FSS structures. The overall thickness of the proposed structure can be as thin as $\lambda/75$, which is the lowest profile reported so far to the authors' knowledge. It has been shown that the transmission and reflection coefficients are almost independent from polarizations and incident angles. A prototype of the second-order bandpass FSS is designed, fabricated and experimentally characterized. The measurement results of this device show a relatively stable frequency response with respect to the angle of incidence up to $\pm 45^\circ$.

The proposed method can also be useful for millimeter wave and terahertz applications, where the substrate loss is dominant in most cases. Such an FSS can be very attractive for a wide range of applications.

REFERENCES

- [1] B. A. Munk, "Frequency selective surfaces theory and design. John Wiley & Sons," New York: Wiley-Interscience, 2000.
- [2] R. Ott, R. Kouyoumjian, and L. Peters, "Scattering by a two-dimensional periodic array of narrow plate," *Radio Science*, vol. 2, no. 11, pp. 1347-1359, 1967.

- [3] B. Munk, and R. Luebbers, "Reflection properties of two-layer dipole arrays," *IEEE Trans. Antennas Propaga.*, vol. 22, no. 6, pp. 766-773, 1974.
- [4] J. C. Vardaxoglou, *Frequency selective surfaces: analysis and design*: Research Studies Press, 1997.
- [5] M. Al-Joumayly, and N. Behdad, "A new technique for design of low-profile, second-order, bandpass frequency selective surfaces," *IEEE Trans. antennas propaga.*, vol. 57, no. 2, pp. 452-459, 2009.
- [6] M. Yan, S. Qu, J. Wang, A. Zhang, L. Zheng, Y. Pang, and H. Zhou, "A miniaturized dual-band FSS with second-order response and large band separation," *IEEE Antennas Wireless Propaga. Lett.*, vol. 14, pp. 1602-1605, 2015.
- [7] M. Gao, S. M. A. M. H. Abadi, and N. Behdad, "A Dual-Band, Inductively Coupled Miniaturized-Element Frequency Selective Surface With Higher Order Bandpass Response," *IEEE Trans. Antennas Propaga.*, vol. 64, no. 8, pp. 3729-3734, 2016.
- [8] M. Gao, S. M. A. M. H. Abadi, and N. Behdad, "A hybrid miniaturized-element frequency selective surface with a third-order bandpass response," *IEEE Antennas Wireless Propaga. Lett.*, vol. 16, pp. 708-711, 2017.
- [9] S. M. A. M. H. Abadi, and N. Behdad, "Inductively-coupled miniaturized-element frequency selective surfaces with narrowband, high-order bandpass responses," *IEEE Trans. Antennas Propaga.*, vol. 63, no. 11, pp. 4766-4774, 2015.
- [10] Matthaei, G.L., Young, L., Jones, E.M.T. "Microwave filters, impedance-matching networks, and coupling structures", Artech House, Inc., Norwood. 1980.
- [11] M. Hussein, J. Zhou, Y. Huang, and B. Al-Juboori, "A Low-Profile Miniaturized Second-Order Bandpass Frequency Selective Surface," *IEEE Antennas Wireless Propaga. Lett.*, vol. 16, pp. 2791-2794, 2017.
- [12] A. I. Zverev, *Handbook of filter synthesis*: Wiley-Blackwell, 2005.
- [13] N. Marcuvitz, *Waveguide handbook*: Iet, 1951.
- [14] C. A. Balanis, *Advanced engineering electromagnetics*: John Wiley & Sons, 1999.